$Ln_2(OH)_5NO_3 \cdot xH_2O$ (Ln = Y, Gd−Lu): A Novel Family of Anion Exchange Intercalation Hosts

Laura J. McIntyre, Lauren K. Jackson, and Andrew M. Fogg*

Department of Chemistry, University of Liverpool, Liverpool, L69 7ZD, United Kingdom

Received July 19, 2007. Revised Manuscript Received October 19, 2007

A class of anion exchangeable layered hydroxides incorporating the smaller lanthanides within the layers has been synthesized via a hydrothermal route. These materials have the composition $Ln_2(OH)_5NO_3 \cdot xH_2O$ (Ln = Y, Gd−Lu; $x \approx 1.5$) and the potential to combine the properties of the lanthanides with the flexibility of intercalation hosts. Powder XRD data suggest that the crystallinity of the Gd phase is lower than that of the other materials, and reactions with the larger lanthanides lead to the formation of other phases, indicating a limiting cationic radius for these materials. The anion exchange capacity of these materials has been shown by facile reactions with a range of organic carboxylate and sulfonate anions, leading to the complete replacement of the nitrate anion.

Introduction

Intercalation reactions have been the focus of numerous investigations over many years due to their potential in modifying and controlling the properties of the host lattice with only a minimal change in structure. One family of layered materials that has received considerable attention is the layered double hydroxides (LDHs), which have found numerous applications in fields as diverse as catalysis[1,2] and shape-selective ion exchange.[3–5] The full range of applications of LDHs was recently reviewed by Feng and Duan.[6] These materials are compositionally flexible in terms of both their layer composition and the range of inorganic and organic anions which can be intercalated between the layers and have the general formula $[M^{2+}_{1-x}M^{3+}_x(OH)_2]^{x+}\text{-}X_{x/n}{}^{n-} \cdot mH_2O$ (e.g., M^{2+} = Mg, Zn, Co, and Ni; M^{3+} = Al, Cr, Fe, and Ga).[1,7,8] Structurally, they are related to brucite ($Mg(OH)_2$) consisting of positively charged layers with exchangeable, charge-balancing anions in the interlayer space.[9] Despite this compositional flexibility, the range of cationic radii which can be incorporated into LDHs is relatively limited, and as such, there have been no reports of lanthanide cations being incorporated into these host lattices, although it has been possible to intercalate lanthanide-containing complexes between the layers.[10]

LDHs are, however, not the only group of hydroxide-based anion exchange host lattices, with the hydroxy double salts (HDSs) and hydroxynitrates attracting growing interest. HDSs can be described using the formulas $(M^{2+}N^{2+})_5(OH)_8(A^{n-})_{2/n}$ and $[(M^{2+}_{1-x}N^{2+}_{1+x})(OH)_{3(1-y)}]^+A(1+3y)/n^{n-}$ where M^{2+} can be Ni^{2+}, Co^{2+}, or Zn^{2+} and occupies octahedral sites within the layers and N^{2+} can be tetrahedrally coordinated Cu^{2+} or Zn^{2+}.[11–14] Analogously to the LDHs, the interlayer anions, typically nitrate, are exchangeable.

The larger lanthanides are known to form layered hydroxynitrates with the general formula $Ln(OH)_2NO_3 \cdot xH_2O$ (Ln = La, Pr, Nd, Sm, and Gd; $x = 0$ and 1),[15–18] and anion exchange has been demonstrated for reactions between $La(OH)_2NO_3 \cdot H_2O$ and acetate, benzoate, and terephthalate salts.[19] Additionally, materials with the composition $Ln_2(OH)_5NO_3 \cdot 2H_2O$ (Ln = Y and Yb)[20–22] have been described with Haschke reporting an orthorhombic unit cell with $a \sim 6.0$ Å, $b \sim 3.8$ Å, and $c \sim 8.5$ Å.[20] The study by Haschke also revealed several related, nonstoichiometric phases with the compositions including $Ln_2(OH)_{5.14}(NO_3)_{0.86}$ (Ln = La, Pr, and Nd) and $Ln_2(OH)_{5.39}(NO_3)_{0.61}$ (Ln = Sm−Dy and Yb) as well as the stoichiometric materials $Ln(OH)_2NO_3$ (Ln = La, Pr, Nd, Sm−Dy).

In this paper, we report the hydrothermal synthesis of some new anion exchange host lattices containing the

* To whom all correspondence should be addressed. Tel.: 44 151 794 2047. Fax: 44 151 794 3587. E-mail: afogg@liverpool.ac.uk.

(1) Cavani, F.; Trifiro, F.; Vaccari, A. *Catal. Today* **1991**, *11*, 173.
(2) Sels, B. F.; De Vos, D. E.; Jacobs, P. A. *Catal. Rev. Sci. Eng.* **2001**, *43*, 443.
(3) Fogg, A. M.; Dunn, J. S.; Shyu, S. G.; Cary, D. R.; O'Hare, D. *Chem. Mater.* **1998**, *10*, 351.
(4) Fogg, A. M.; Green, V. M.; Harvey, H. G.; O'Hare, D. *Adv. Mater.* **1999**, *11*, 1466.
(5) Ragavan, A.; Khan, A.; O'Hare, D. *J. Mater. Chem.* **2006**, *16*, 4155.
(6) Feng, L.; Duan, X. *Struct. Bonding (Berlin)* **2006**, *119*, 193.
(7) Khan, A. I.; O'Hare, D. *J. Mater. Chem.* **2002**, *12*, 3191.
(8) Williams, G. R.; O'Hare, D. *J. Mater. Chem.* **2006**, *16*, 3065.
(9) Allman, R. *Chimia* **1970**, *24*, 99.
(10) Gago, S.; Pillinger, M.; Ferreira, R. A. S.; Carlos, L. D.; Santos, T. M.; Goncalves, I. S. *Chem. Mater.* **2005**, *17*, 5803.
(11) Kandare, E.; Hossenlopp, J. M. *J. Phys. Chem. B* **2005**, *109*, 8469.
(12) Kasai, A.; Fujihara, S. *Inorg. Chem.* **2006**, *45*, 415.
(13) Meyn, M.; Beneke, K.; Lagaly, G. *Inorg. Chem.* **1990**, *29*, 5201.
(14) Stahlin, W.; Oswald, H. R. *Acta Crystallogr, Sect. B* **1970**, *26*, 860.
(15) Louer, D.; Louer, M. *J. Solid State Chem.* **1987**, *68*, 292.
(16) Louer, M.; Louer, D.; Delgado, A. L.; Martinez, O. G. *Eur. J. Solid State Inorg. Chem.* **1989**, *26*, 241.
(17) Lundberg, M.; Skarnulis, A. J. *Acta Crystallogr., Sect. B* **1976**, *32*, 2944.
(18) Mullica, D. F.; Sappenfield, E. L.; Grossie, D. A. *J. Solid State Chem.* **1986**, *63*, 231.
(19) Newman, S. P.; Jones, W. *J. Solid State Chem.* **1999**, *148*, 26.
(20) Haschke, J. M. *Inorg. Chem.* **1974**, *13*, 1812.
(21) Holcombe, C. E. *J. Am. Ceram. Soc.* **1978**, *61*, 481.
(22) Schildermans, I.; Mullens, J.; Yperman, J.; Franco, D.; Vanpoucke, L. C. *Thermochim. Acta* **1994**, *231*, 185.

10.1021/cm7019284 CCC: $40.75
Published on Web 12/05/2007

smaller lanthanide cations, with the composition $Ln_2(OH)_5NO_3 \cdot 1.5H_2O$ (Ln = Y, Gd−Lu), and demonstrate their anion exchange capacity. These materials have the potential to combine the properties of the lanthanides, for example, optical and catalytic, with the flexibility of intercalation hosts.

Experimental Section

Synthesis. The $Ln_2(OH)_5NO_3 \cdot xH_2O$ (Ln = Y, Gd−Lu) phases are synthesized via a hydrothermal route. In a typical reaction, 7.5 mL of a 0.44 M $Ln(NO_3)_3 \cdot xH_2O$ aqueous solution is added to 2.5 mL of an aqueous solution containing 2.10 M NaOH and 1.44 M $NaNO_3$ and treated hydrothermally at 150 °C (125 °C for Y) for 48 h. The resulting solid was filtered, washed, and allowed to dry in the air.

Anion exchange reactions were performed between the $Ln_2(OH)_5NO_3 \cdot xH_2O$ (Ln = Y, Gd−Lu) phases and an aqueous solution containing a 3-fold molar excess of a range of (di)sodium salts of organic anions at room temperature. The anions investigated were maleate, fumarate, phthalate, terephthalate, oxalate, malonate, succinate, glutarate, suberate, decylsulfonate, dodecylsulfate, 2,6-naphthalenedisulfonate (NDS), and 2,6-anthraquinonedisulfonate (AQDS). All of the chemicals were supplied by Aldrich and used without further purification.

Characterization. Powder X-ray diffraction patterns were recorded with Cu $K\alpha_1$ radiation on a Stoe Stadi-P diffractometer in either Bragg–Brentano or Debye–Scherrer geometry. Samples for transmission electron microscopy (TEM) analysis were prepared by suspending a fine suspension in ethanol before deposition onto a holey carbon grid. Selected area electron diffraction patterns were recorded on a JEOL 2000 FX transmission electron microscope equipped with a double tilting goniometer stage (±30°). The compositions of the materials were determined by a combination of thermogravimetric analysis (TGA) and elemental analysis. TGA was performed using a Seiko SII-TG/DTA 6300 thermal analyzer. The metal content of the materials was found by inductively coupled plasma analysis on a Ciros CCD optical emission spectrometer following complete dissolution of the samples in dilute HNO_3, and CHN analysis was performed on a FlashEA 1112 instrument. Fourier transform infrared (FTIR) spectra were obtained using a Nicolet Nexus FT-IR spectrophotometer.

Results and Discussion

A novel family of hydroxynitrates, containing the smaller lanthanide cations, has been prepared as crystalline materials by a hydrothermal synthesis. The composition of the materials was determined to be $Ln_2(OH)_5NO_3 \cdot xH_2O$ (Ln = Y, Gd−Lu; $x \approx 1.5$) by elemental analysis and TGA, and the characterizing data are summarized in Table 1. As these materials are isostructural and have comparable analytical data, they will be exemplified here by the Er phase with data on the other compounds provided in the Supporting Information. The TGA data, shown in Figure 1 for $Er_2(OH)_5NO_3 \cdot .xH_2O$, display three distinct mass losses comparable to those seen for other layered hydroxides. The first mass loss of 4.35% (calculated value for $x = 1.5$ is 5.21%) below 150 °C corresponds to the loss of cointercalated water. This is followed by the partial decomposition of the layers, resulting in a mass loss of 7.24% (7.19%) by 350 °C, leaving a material of nominal composition "$Er_2O_2(OH)NO_3$".[22] Complete decomposition to Er_2O_3 occurs by 650 °C with a further mass loss of 11.68% (12.39%). No further mass loss is observed above 650 °C.

Table 1. Characterizing Data for the New Layered Lanthanide Hydroxides, $Ln_2(OH)_5NO_3 \cdot xH_2O$

Ln	composition	interlayer separation (Å)	elemental analysis observed (%)	elemental analysis calculated (%)
Y	$Y_2(OH)_5NO_3 \cdot 1.5H_2O$	9.18	Y (49.89) N (3.91) H (2.25)	Y (50.53) N (3.98) H (2.29)
Tb	$Tb_2(OH)_5NO_3 \cdot 1.5H_2O$	9.06	Tb (62.66) N (2.55) H (1.53)	Tb (64.61) N (2.85) H (1.64)
Dy	$Dy_2(OH)_5NO_3 \cdot 1.5H_2O$	9.06	Dy (63.71) N (3.00) H (1.55)	Dy (65.12) N (2.81) H (1.62)
Ho	$Ho_2(OH)_5NO_3 \cdot 1.5H_2O$	9.10	Ho (59.89) N (2.34) H (1.45)	Ho (65.46) N (2.78) H (1.60)
Er	$Er_2(OH)_5NO_3 \cdot 1.5H_2O$	9.28	Er (65.20) N (2.82) H (1.54)	Er (65.77) N (2.75) H (1.59)
Tm	$Tm_2(OH)_5NO_3 \cdot 1.5H_2O$	9.14	Tm (60.55) N (2.46) H (1.39)	Tm (65.99) N (2.73) H (1.58)

These new phases comprise microcrystalline powders and display an approximately hexagonal platelike morphology, as can be seen from the SEM image of $Y_2(OH)_5NO_3 \cdot xH_2O$ in Figure 2. The phase purity of these materials has been confirmed by powder XRD for the samples with Ln = Y, Tb−Tm, while those with Gd, Yb, and Lu always contain impurities. A typical powder XRD pattern, for $Er_2(OH)_5NO_3 \cdot xH_2O$, is shown in Figure 3, from which a series of strong (00*l*) reflections is apparent, characteristic of a layered phase and corresponding to an interlayer separation of 9.28 Å. Additionally, and in contrast to many other layered hydroxides, there are a significant number of relatively weak non-(00*l*) reflections observed, indicating that the layers are ordered. This order within the *ab* plane is confirmed by electron diffraction. The TEM image shown in Figure 4 indicates lattice parameters of $a \sim 7.1$ Å and $b \sim 12.7$ Å and reveals that there are no systematic absences for this plane. It was, however, not possible to observe diffraction from along the *c* axis. Tilting of the samples produced little change in the diffraction patterns, and this is indicative of extensive layer stacking faults within the crystal along the *c* axis, as has been observed in other layered systems.[23] The disorder inherent in these materials has so far prevented a full structure determination from powder XRD data, and despite extensive optimization of the reaction conditions through variation of reagent concentrations, reaction temperature, and time and control of the cooling rate, it has not proved possible to obtain diffraction-quality single crystals of any of these phases. The *a* and *b* parameters observed by electron diffraction combined with the interlayer separation show that these materials are structurally different from the orthorhombic ones reported by Haschke previously (a = 6.064(4) Å, b = 3.800(1) Å, and c = 8.533(3) Å for $Y_2(OH)_5NO_3 \cdot 2H_2O$), confirming the possibility of polymorphism in this system or suggesting that small changes in the

(23) Fogg, A. M.; Meldrum, J.; Darling, G. R.; Claridge, J. B.; Rosseinsky, M. J. *J. Am. Chem. Soc.* **2006**, *128*, 10043.

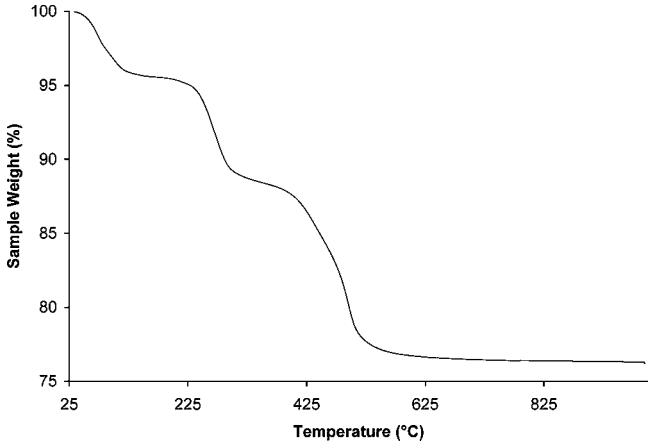

Figure 1. TGA trace for $Er_2(OH)_5NO_3 \cdot xH_2O$ showing mass losses of 4.35% below 150 °C and further mass losses of 7.24% by 350 °C and 11.68% by 650 °C.

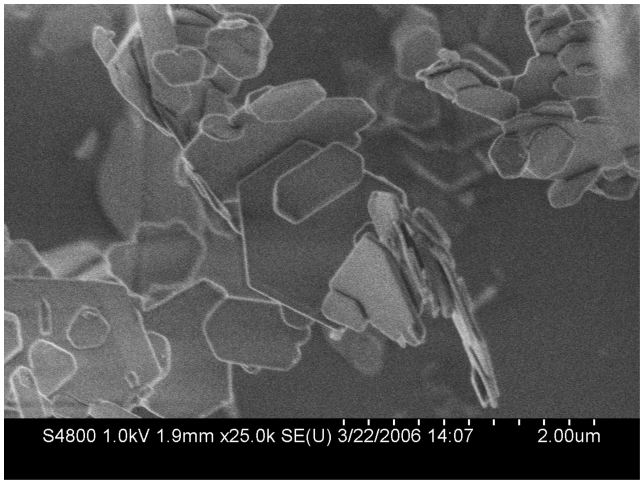

Figure 2. SEM image of $Y_2(OH)_5NO_3 \cdot xH_2O$.

composition through different hydration levels can have a significant effect on the structure. Further evidence for this comes from the fact that it has not proved possible to synthesize the Yb- and Lu-containing materials phase-pure. In both cases, a second phase displaying a slightly larger interlayer separation of approximately 9.40 Å is apparent in the powder XRD data. Analysis of the bulk material via TGA and elemental analysis suggests that these two phases have similar compositions and are therefore different from the related phases reported by Haschke,[20] as there is little deviation from the expected analysis for the pure $Ln_2(OH)_5NO_3 \cdot xH_2O$ phases. As a result, these host lattices will not be discussed further in this paper.

Powder X-ray diffraction data indicate that $Gd_2(OH)_5NO_3 \cdot xH_2O$ is less crystalline than the other materials, suggesting that Gd marks the limiting cation size for this phase. In addition, a small amount of an impurity phase, possibly $GdONO_3$, is always present in the sample. Reactions with the larger lanthanides under the same conditions yield a mixture of the oxide, $Ln(OH)_2NO_3 \cdot xH_2O$, and $Ln(OH)_3$ as products with the precise combination dependent on the lanthanide used.

It is likely that the structure of these $Ln_2(OH)_5NO_3 \cdot xH_2O$ materials is related to the $[Ln_4(OH)_{10}(H_2O)_4]A$ (Ln = Y, Dy, Ho, and Yb; A = 2,6-naphthalenedisulfonate and 2,6-anthraquinonedisulfonate) phases recently reported by Gándara et al.[24] Single crystal diffraction studies revealed an orthorhombic structure for the Y-2,6-naphthalenedisulfonate (a = 12.639(1) Å, b = 30.525(2) Å, and c = 7.1348(6) Å) and Yb-2,6-anthraquinonedisulfonate materials with lattice parameters comparable to those seen in this work for the nitrate materials. In these materials, the positively charged $[Ln_4(OH)_{10}(H_2O)_4]^{2+}$ layers contain lanthanide cations which are 8- and 9-coordinated to μ_3-hydroxy groups and one water molecule giving rise to two different polyhedra: a dodecahedron and a monocapped square antiprism. The organic anions are located between the layers and are ordered through hydrogen-bonding interactions with the layers. Despite the similarity in lattice parameters, it has not, however, proved possible to index the powder diffraction data of the $Ln_2(OH)_5NO_3 \cdot xH_2O$ materials on an orthorhombic cell, requiring instead a monoclinic one with $a \sim 7.1$ Å, $b \sim 12.7$ Å, $c \sim 18.8$ Å, and $\beta \sim 92.5°$.

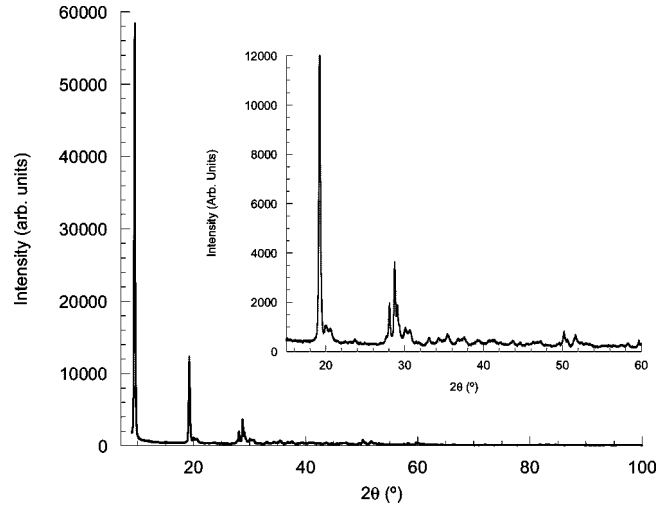

Figure 3. Powder X-ray diffraction pattern of $Er_2(OH)_5NO_3 \cdot xH_2O$.

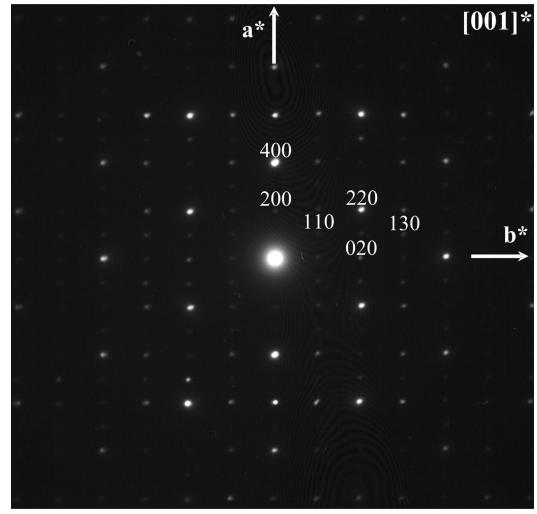

Figure 4. Selected area electron diffraction pattern of $Er_2(OH)_5NO_3 \cdot xH_2O$.

(24) Gándara, F.; Perles, J.; Snejko, N.; Iglesias, M.; Gomez-Lor, B.; Gutierrez-Puebla, E.; Monge, M. A. *Angew. Chem., Int. Ed.* **2006**, *45*, 7998.

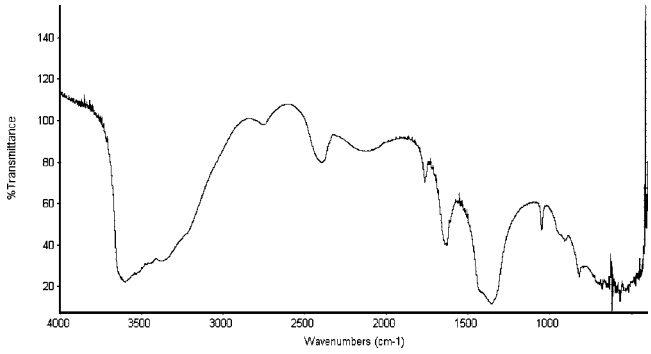

Figure 5. FTIR spectrum of $Er_2(OH)_5NO_3 \cdot xH_2O$.

The FTIR spectrum of $Er_2(OH)_5NO_3 \cdot xH_2O$ is shown in Figure 5 and is representative of all of the host materials (see the Supporting Information). From the data, it can be seen that there is a broad band at approximately 1370 cm^{-1}, which is characteristic of an uncoordinated nitrate anion and is comparable to observations made on other layered hydroxides containing interlayer nitrate groups.[19,25] Additionally, this supports the structural model proposed above in which the nitrate is located between the $[Er_2(OH)_5]^+$ layers rather than coordinated to the lanthanide cation as is observed in $La(OH)_2NO_3 \cdot H_2O$.[16] The other features in the spectrum are a broad absorption band at approximately 3500 cm^{-1} corresponding to a combination of the stretching vibrations of the layer hydroxyl groups and the interlayer water molecules and a bending vibration of water at 1630 cm^{-1}.

The characterizing data discussed above for the $Ln_2(OH)_5NO_3 \cdot xH_2O$ (Ln = Y, Gd−Lu) phases are consistent with the formation of layered hydroxynitrates which incorporate the smaller lanthanide cations within the layers and have charge balancing nitrate anions between them.

One characteristic property of the LDHs and other layered hydroxides is the ability to undergo anion exchange reactions with a variety of inorganic and organic anions. For the $Ln_2(OH)_5NO_3 \cdot xH_2O$ (Ln = Y, Gd−Lu) phases, anion exchange has been demonstrated with a range of organic carboxylates and sulfonates for all of the host lattices. In the majority of cases, the reactions are facile, occurring at room temperature in a few minutes. Complete anion exchange was confirmed by the absence of reflections characteristic of the host lattice in the powder XRD patterns and of nitrogen in the elemental analysis. In a couple of the reactions, typically with smaller anions such as oxalate and malonate, anion exchange proved to be incomplete, so formulas containing both nitrate and the organic anion are reported. Successful anion exchange reactions, yielding $Ln_2(OH)_5A_{0.5} \cdot xH_2O$ ($x \approx 1.5$) for dianions, have been observed with dicarboxylates, including succinate, suberate, fumarate, maleate, phthalate, and terephthalate, and sulfonates, for example, decylsulfonate and 2,6-naphthalenedisulfonate. Typical powder X-ray diffraction patterns of the anion exchange derivatives of $Er_2(OH)_5NO_3 \cdot xH_2O$ are shown in Figure 6, and the characterizing data for the materials are summarized in Table 2. FTIR spectra of the anion exchange

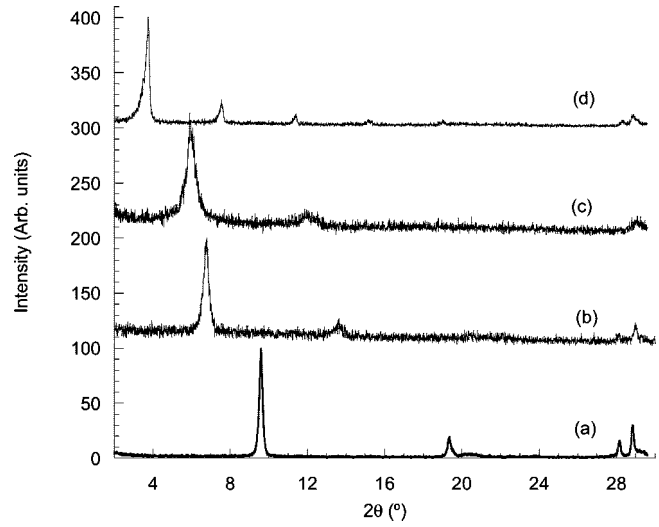

Figure 6. Powder XRD diffraction patterns of (a) $Er_2(OH)_5NO_3 \cdot xH_2O$ and the anion exchange intercalation compounds (b) $Er_2(OH)_5(p\text{-}C_6H_4(CO_2)_2)_{0.5} \cdot xH_2O$, (c) $Er_2(OH)_5(C_8H_{12}O_4)_{0.5} \cdot xH_2O$, and (d) $Er_2(OH)_5(C_{10}H_{21}OSO_3) \cdot xH_2O$.

products (see the Supporting Information) show the loss of bands due to the nitrate and the appearance of symmetric and asymmetric COO^- stretches from the organic anions (1570 and 1400 cm^{-1}, respectively), providing further evidence of successful reactions.[26] From the data, it can be seen that these are very flexible hosts in their exchange reactions with organic anions, being able to accommodate small anions with little increase in the interlayer separation, or in the case of oxalate a decrease, and large surfactant anions where there is up to a 3-fold increase in the interlayer separation relative to the host. Additional characterization by TGA indicates that the thermal behavior of these intercalation compounds is similar to that of comparable organic derivatives of LDHs. Depending on the nature of the organic anion, the TGA traces comprise two or three distinct regions of mass loss, and representative data sets are included in the Supporting Information. The first corresponds to the removal of cointercalated water below 150 °C followed by the dehydroxylation of the layers and decomposition of the guest anions leaving Ln_2O_3.

The ease of anion exchange in the $Ln_2(OH)_5NO_3 \cdot xH_2O$ materials contrasts with the more forcing conditions of prolonged heating at 65 °C required to bring about complete anion exchange for $La(OH)_2NO_3 \cdot H_2O$.[19] It is likely that this difference reflects differing nitrate environments in the two host lattices. In $La(OH)_2NO_3 \cdot H_2O$, the nitrate anion is directly coordinated to the La^{3+} cation,[16] and by analogy to the $[Ln_4(OH)_{10}(H_2O)_4]A$ (Ln = Y, Dy, Ho, and Yb; A = 2,6-naphthalenedisulfonate and 2,6-anthraquinonedisulfonate)[24] phases, it is likely that in the host materials reported here the nitrate is uncoordinated in the interlayer gallery, permitting more facile exchange reactions. A comparison of the interlayer separations of the terephthalate intercalates of both families (12.9 Å for $La(OH)_2(p\text{-}C_8H_4O_4)_{0.5} \cdot H_2O$ and 13.1 Å for $Er_2(OH)_5(p\text{-}C_8H_4O_4)_{0.5} \cdot H_2O$) indicates that the layer thickness is comparable in the different host lattices,

(25) Fogg, A. M.; Williams, G. R.; Chester, R.; O'Hare, D. *J. Mater. Chem.* **2004**, *14*, 2369.

(26) Li, F.; Zhang, F. H.; Evans, D. G.; Forano, C.; Duan, X. *Thermochim. Acta* **2004**, *424*, 15.

Table 2. Characterizing Data for the Organic Anion Exchange Derivatives of $Er_2(OH)_5NO_3 \cdot xH_2O$

anion	composition	interlayer separation (Å)	elemental analysis	
			observed (%)	calculated (%)
maleate	$Er_2(OH)_5(cis\text{-}C_4H_2O_4)_{0.5} \cdot 1.5H_2O$	9.4	Er (65.25), C (4.93), H (1.76)	Er (66.42), C (4.77), H (1.80)
fumarate	$Er_2(OH)_5(trans\text{-}C_4H_2O_4)_{0.5} \cdot 1.5H_2O$	9.6	Er (65.90), C (4.66), H (1.78)	Er (66.42), C (4.77), H (1.80)
phthalate	$Er_2(OH)_5(o\text{-}C_8H_4O_4)_{0.5} \cdot H_2O$	14.0	Er (58.87), C (8.99), H (2.08)	Er (63.16), C (9.24), H (1.75)
terephthalate	$Er_2(OH)_5(p\text{-}C_8H_4O_4)_{0.5} \cdot H_2O$	13.1	Er (58.87), C (9.42), H (2.06)	Er (63.16), C (9.24), H (1.75)
malonate	$Er_2(OH)_5(C_3H_2O_4)_{0.5} \cdot 1.5H_2O$	11.2	Er (66.91), C (3.64), H (1.80)	Er (67.23), C (3.62), H (1.82)
succinate	$Er_2(OH)_5(C_4H_4O_4)_{0.5} \cdot 1.5H_2O$	9.8	Er (66.07), C (4.68), H (1.98)	Er (66.29), C (4.76), H (1.99)
glutarate	$Er_2(OH)_5(C_5H_6O_4)_{0.5} \cdot 1.5H_2O$	10.4	Er (63.68), C (6.00), H (2.21)	Er (65.38), C (5.87), H (2.17)
suberate	$Er_2(OH)_5(C_8H_{12}O_4)_{0.5} \cdot H_2O$	14.8	Er (60.80), C (10.12), H (2.70)	Er (62.80), C (9.17), H (2.50)
decylsulfonate	$Er_2(OH)_5(C_{10}H_{21}SO_4) \cdot 1.5H_2O$	23.9	Er (50.37), C (17.52), H (4.20)	Er (48.91), C (17.56), H (4.27)
NDS	$Er_2(OH)_5(C_{10}H_6(SO_3)_2)_{0.28}(NO_3)_{0.44} \cdot 3H_2O$	15.6	Er (57.19), C (4.69), H (1.64), N (0.73)	Er (57.57), C (5.78), H (2.19), N (1.06)
AQDS	$Er_2(OH)_5(C_{14}H_6O_2(SO_3)_2)_{0.22}(NO_3)_{0.54} \cdot 3H_2O$	18.2	Er (55.46), C (5.14), H (1.63), N (1.10)	Er (56.74), C (6.27), H (2.10), N (1.35)

with the slightly smaller value observed for $La(OH)_2(p\text{-}C_8H_4O_4)_{0.5} \cdot H_2O$ suggesting the coordination of the anion to the La^{3+}cation in that system.

From an analysis of the interlayer separations of the aliphatic dicarboxylate intercalates ($Ln_2(OH)_5(OOC(CH_2)_n\text{-}COO)_{0.5} \cdot xH_2O$; n = 0–6), it is possible to infer the orientation of the guest anions between the layers. The plot of interlayer separation against the number of CH_2 groups in the chain, n, is shown in Figure 7 for the Er compounds and indicates a roughly linear relationship between the gallery height and the chain length. The gradient of the plot is 1.07 Å/C atom, which can be compared with the linear intercarbon distance along the chain of 1.27 Å, indicating the formation of a monolayer of anions in the interlayer gallery and allowing a tilting angle of 58° to be calculated. The tilt angles decrease across the series varying from 82° for Tb to 51° for the Tm host. From the schematic orientation shown in the inset of Figure 7, it can be seen that this orientation is likely to maximize the electrostatic interactions between the host layers and the guest anions, and these tilt angles are comparable to those seen in similar LDH systems.[27,28]

Anion exchange reactions have also been performed with NDS and AQDS in order to permit a comparison with the phases reported by Gándara et al.[24] These anion exchange reactions, with the Y and Er host lattices, proved to be incomplete in the majority of cases, with significant amounts of N being detected in the elemental analysis. XRD data showed that the products consist of an unreacted host lattice and an expanded phase with interlayer separations of around 15.6 Å for the NDS materials and 18.2 Å for the AQDS phases, compared with the published values of 15.26 and 17.83 Å, respectively. In both cases, the anion exchange materials have interlayer separations which are slightly larger than those prepared hydrothermally by Gándara et al. It is likely that these differences result from variations in the orientation of the guest anion due to variations in the degree of hydration rather than from significant differences in the layer structure, which retains the composition $[Ln_2(OH)_5]^+$ after exchange. In order to confirm this, the materials were also synthesized following the method reported by Gandara et al., giving rise to phases with the same interlayer separation as those prepared by anion exchange. Powder XRD data for $Y_2(OH)_5(NDS)_{0.5} \cdot xH_2O$ prepared hydrothermally and by anion exchange are shown for comparison in Figure 8, from which it is clear that the same material is prepared via both

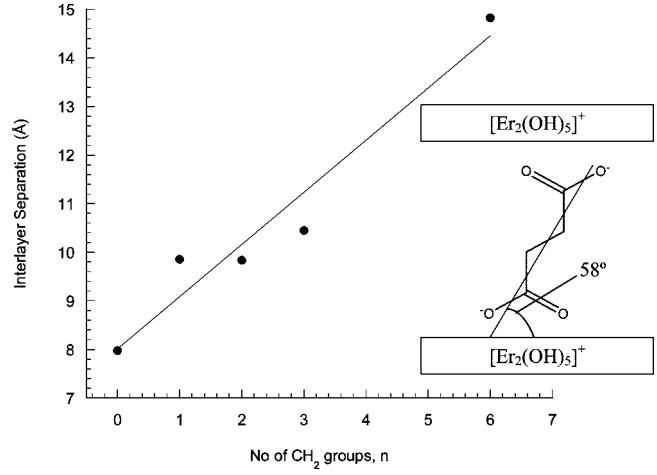

Figure 7. Plot of interlayer separation against the number of CH_2 groups, n, in the aliphatic chain of some dicarboxylate intercalates, $Er_2(OH)_5(OOC(CH_2)_nCOO)_{0.5} \cdot xH_2O$. Inset: Schematic representation of the succinate intercalate of $Er_2(OH)_5NO_3 \cdot xH_2O$ indicating the orientation of the guest anions between the layers.

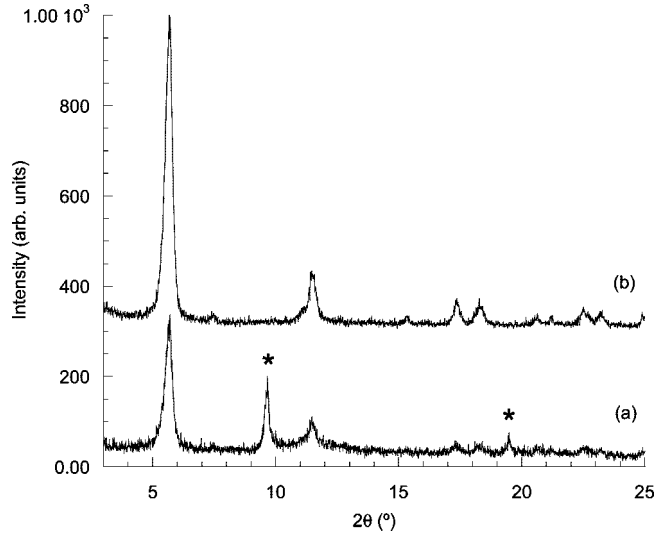

Figure 8. Powder XRD diffraction patterns of $Y_2(OH)_5(NDS)_{0.5} \cdot xH_2O$ prepared (a) by anion exchange and (b) hydrothermally. The asterisks indicate unreacted $Y_2(OH)_5NO_3 \cdot xH_2O$ in the anion exchange sample.

(27) Borja, M.; Dutta, P. K. *J. Phys. Chem.* **1992**, *96*, 5434.
(28) Williams, G. R.; Dunbar, T. G.; Beer, A. J.; Fogg, A. M.; O'Hare, D. *J. Mater. Chem.* **2006**, *16*, 1222.

routes and that the hydrothermal synthesis is a more efficient route to these particular compounds. Characterizing data for these phases is included in Table 2 and the Supporting Information.

Preliminary optical measurements on the nitrate host lattices revealed very weak fluorescence for the Tb and Dy materials. Experiments to form solid solutions of the host lattices leading to materials containing a more dilute dispersion of the optically interesting cations are ongoing along with attempts to dope the larger lanthanides, for example, Eu into the existing hosts. Full details of these materials will be reported elsewhere.

Conclusions

We have synthesized and characterized a family of anion exchange intercalation hosts with the generalized formula $Ln_2(OH)_5NO_3 \cdot xH_2O$ (Ln = Y, Gd−Lu; $x \approx 1$–1.5) via a hydrothermal route. These are the first such materials to contain the smaller lanthanide cations within the host layers, giving them the potential to combine the catalytic and optical properties of the lanthanides with the flexibility of intercalation hosts. These intercalation hosts have been shown to undergo facile exchange reactions with a wide range of organic carboxylate and sulfonate anions.

Acknowledgment. We thank Dr. Mathieu Allix for the microscopy and EPSRC for funding under EP/D060664/1. A.M.F. thanks the Royal Society for a University Research Fellowship.

Supporting Information Available: Characterizing data (XRD, TGA, FTIR, and elemental analysis) on the hosts and the anion exchange derivatives reported in this paper are provided. This information is available free of charge via the Internet at http://pubs.acs.org.

CM7019284